


Article

Experimental Investigation of High Speed Cross-Domain Vehicles with Hydrofoil

Zeqi Shi ¹, Xiangkui Tan ², Yiwei Wang ³, Pengyu Lv ^{1,2}, Yong Zou ¹, Xia Wan ², Kai Lv ², Bingzhen Li ¹, Huiling Duan ^{1,2,4} and Hongyuan Li ^{1,2,4,*} 

¹ Nanchang Innovation Institute of Peking University, Nanchang 330096, China

² State Key Laboratory for Turbulence and Complex Systems, Department of Mechanics and Engineering Science, BIC-ESAT, College of Engineering, Peking University, Beijing 100871, China

³ Key Laboratory for Mechanics in Fluid Solid Coupling Systems, Institute of Mechanics, Chinese Academy of Sciences, Beijing 100190, China

⁴ CAPT, HEDPS and IFSA Collaborative Innovation Center of MoE, Peking University, Beijing 100871, China

* Correspondence: lihongyuan@pku.edu.cn; Tel.: +86-159-0107-2733

Abstract: Unmanned equipment, such as unmanned underwater vehicles (UUVs) and unmanned surface vehicles (USVs), are widely used in marine science for underwater observation, rescue, military purposes, etc. However, current vehicles are not applicable in complex cross-domain scenarios, because they can only perform well in either surface navigation or underwater diving. This paper deals with the design and fabrication of a cross-domain vehicle (CDV) with four hydrofoils that can both navigate at high speed on the surface, like a USV and dive silently underwater, like a UUV. The CDV's propulsion is provided by a water jet propeller and its dive is achieved by a vertical propeller. The effect of hydrofoils and the performance of the CDV were tested and characterized in experiments, which showed that the hydrofoils improved the stability and surface sailing speed of the CDV. The maximum speed of the CDV was up to 14 kn, which is the highest of its kind according to current knowledge. This work confirmed the feasibility of high-performance CDVs and provided useful information for further improvements to the design.

Keywords: cross-domain vehicles; high speed; hydrofoil; water jet propeller; vertical propeller



Citation: Shi, Z.; Tan, X.; Wang, Y.; Lv, P.; Zou, Y.; Wan, X.; Lv, K.; Li, B.; Duan, H.; Li, H. Experimental Investigation of High Speed Cross-Domain Vehicles with Hydrofoil. *J. Mar. Sci. Eng.* **2023**, *11*, 152. <https://doi.org/10.3390/jmse11010152>

Academic Editor: Alessandro Ridolfi

Received: 5 December 2022

Revised: 23 December 2022

Accepted: 30 December 2022

Published: 8 January 2023



Copyright: © 2023 by the authors. Licensee MDPI, Basel, Switzerland. This article is an open access article distributed under the terms and conditions of the Creative Commons Attribution (CC BY) license (<https://creativecommons.org/licenses/by/4.0/>).

1. Introduction

Unmanned surface vehicles (USVs) and unmanned underwater vehicles (UUVs) require less time, labor and resources and thus hold more potential in marine science [1]. These unmanned vehicles are platforms carrying different observation and operation equipment, providing more accurate ocean observation [2], more extensive ocean exploration [3] and more efficient underwater engineering [4,5]. However, traditional USVs can only sail on the ocean surface, limiting their ability to observe underwater targets. Traditional UUVs do not perform well in rapid large-range exploration missions, because of their low speeds and difficulties in cross-domain communication. Recently, researchers developed a collaborative team of heterogeneous vehicles. The collaborative team can perform more complex monitoring and engineering tasks such as monitoring coral reefs [6–8], tracking multiple targets underwater [9,10] and obtaining a multi-domain awareness of a floating structure [11–13]. However, it is difficult and costly to harmoniously integrate heterogeneous vehicles into one team and organizing and controlling such a system is more difficult.

Lately, researchers have conducted several studies on hybrid unmanned vehicles that combine USVs and UUVs. Jin et al. [14] proposed a hybrid vehicle, which is a USV connected with a UUV through cables. Chen et al. [15] developed an unmanned semi-submersible vehicle, which can carry out autonomous navigation in complex sea conditions. Olmo et al. [16] designed a vehicle with UUV and USV characteristics that can navigate

on the surface and underwater. Vehicle dives are achieved by generating down force in the wings. Zheng et al. [17] designed a surface planning submersible ship. This is a new multi-state ship which can sail at high speed on the surface in the planning mode and cruise underwater at low speed. A novel ballast channel system is developed to provide a quick and easy submerge-emerge process. Ueno et al. [18,19] proposed a new concept submersible surface ship that can escape from rough seas by diving underwater using downward lift of wings. Huo et al. [20] proposed a submersible high-speed craft, which is characterized by rapid switching among underwater, semi-underwater and surface navigation modes. The switching is achieved by two pairs of wings and novel ballast channels, which can change the vertical and longitudinal components of the hydrodynamic forces and moments. Cong et al. [21] proposed a submersible multi-state vehicle, realizing underwater and surface navigation.

Generally speaking, the above hybrid unmanned vehicles are only realized by simulations and model experiments and there are no reports on CDVs in reality. In addition, the propulsion efficiency of all the above hybrid unmanned vehicles is insufficient to satisfy the requirements of practical navigation.

Hydrofoils are widely used in surface vehicles for better propulsion efficiency. A hydrofoil is a lifting surface or foil, that operates in water. When a hydrofoil craft gains speed, the hydrofoils lift the hull out of the water, decreasing drag and allowing greater speeds. The effect of hydrofoil structures on aircraft was studied as early as 1973 [22]. Garg et al. [23] optimized the hydrofoil and successfully tested it on a hydrofoil craft. Budiyo et al. [24] designed a variable-position hydrofoil to enable high-speed navigation. Suastika et al. [25] conducted a seakeeping analysis of hydrofoil craft and found that the seakeeping of catamarans improved significantly after adding hydrofoils. These advantages of hydrofoil crafts in speed and stability inspired us to design a CDV with hydrofoils.

In this paper, a brand-new design of a CDV is presented. A prototype named Qianxiang I was fabricated and its performance was experimentally tested and characterized. The work presented in this paper has three innovative achievements:

First, this paper designed and fabricated a new CDV that uses a water jet propeller to provide propulsion. This vehicle can sail at high speed on the water surface and navigate silently underwater.

Second, this paper designed a set of hydrofoils for the CDV, which greatly increased the surface speed to 14 kn and improved the navigation stability.

Finally, the performance of CDV was experimentally characterized, proving the feasibility of the high-performance CDV and benefiting from an understanding of the mechanism of the multi-state transition process.

The rest of the paper is organized as follows. Section 2 elaborates the concept and design principles of the CDV. Section 3 explains the fabrication of the CDV in terms of four subsystems. Section 4 characterizes the performance of the CDV in different navigation states. Section 5 discusses the experimental shortcomings and outlook. Finally, conclusions are drawn in Section 6.

2. The Concept and Design Principles of CDV

CDV integrates the concepts of UUV and USV and can navigate both on the surface and underwater according to different mission requirements. The CDV is composed of a main body structure, hydrofoils, a rudder and stable rudders. Figure 1 shows the CDV, Qianxiang I.

Figure 2 shows schematic sketches of the attitudes and the submerge-emerge process of the CDV when it sails on the surface, dives, navigates underwater, floats upward and moves at high speed on the surface. Figure 2c demonstrates the movements of the CDV in a cross-domain process. The detailed force analysis of the vehicle is shown in Figure 2a–e. The variable definitions are shown in Table 1.

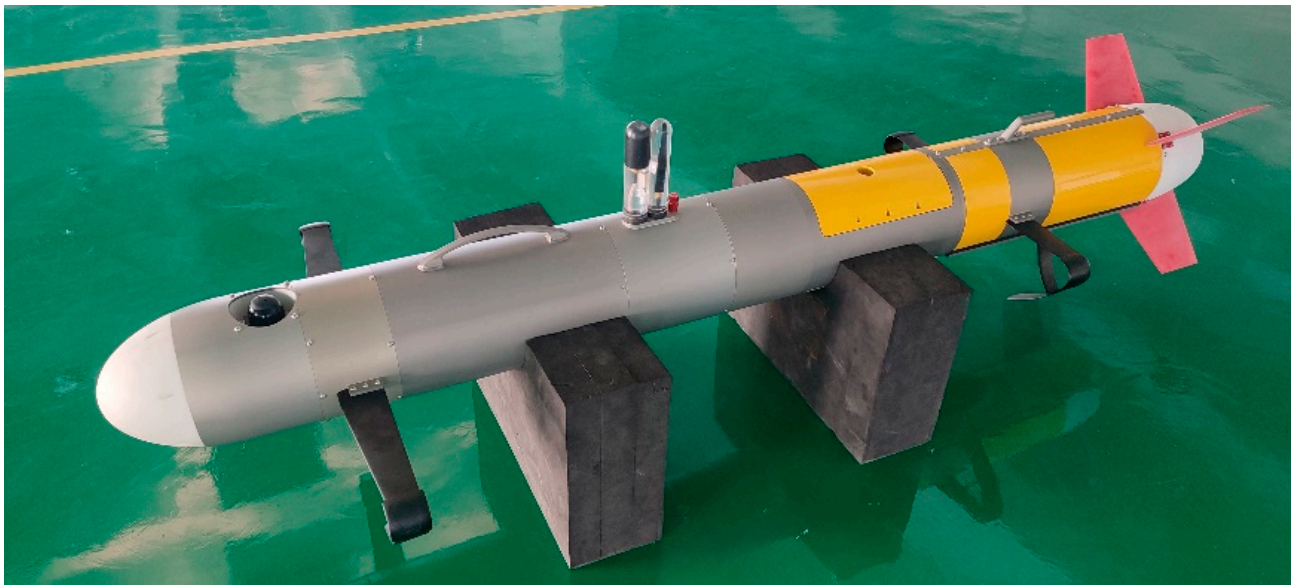


Figure 1. The CDV, Qianxiang I.

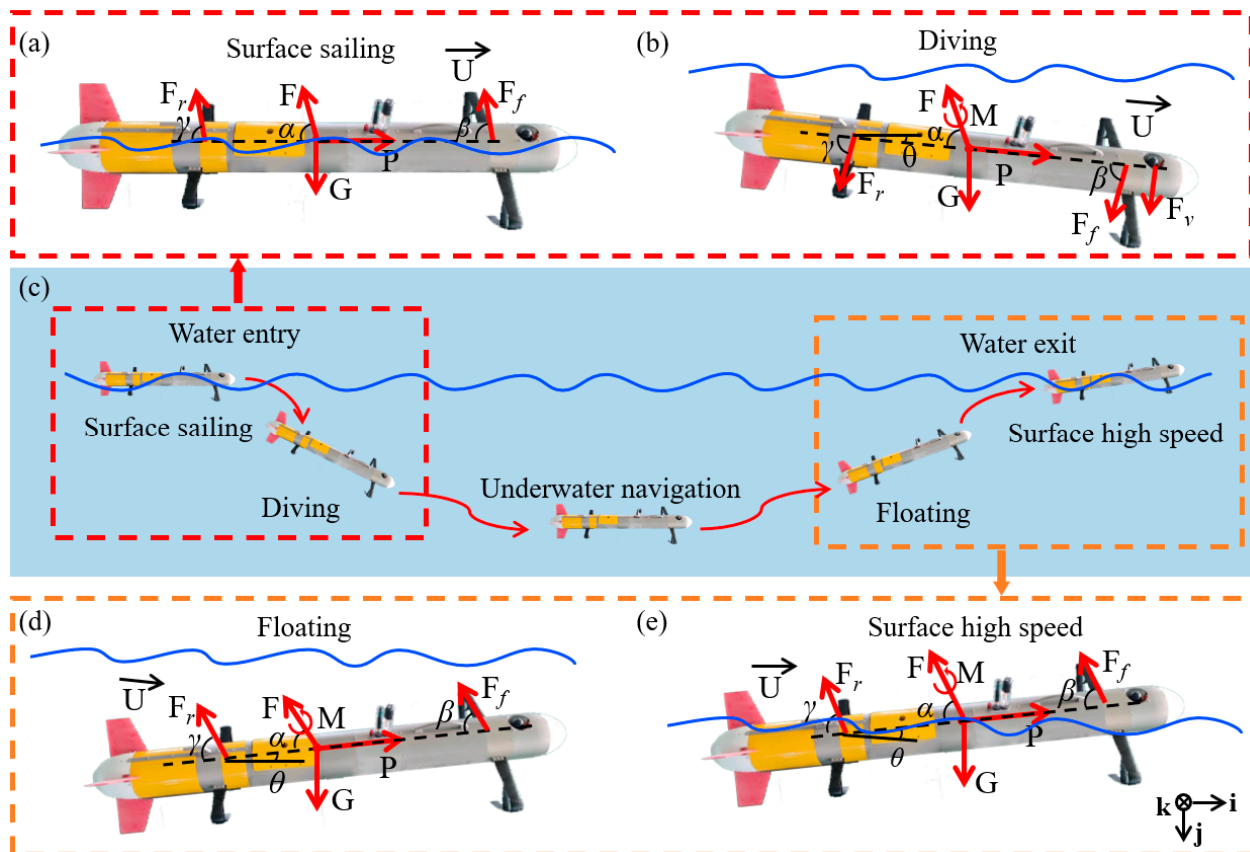


Figure 2. Schematic sketches of the attitudes and the submerge-emerge process of the CDV when it sails on the surface, dives, navigates underwater, floats upward and moves at high speed on the surface. The global coordinate system is located in the lower right corner. The blue wavy line represents the water surface. (a) Force analysis of the CDV on surface sailing. (b) Force analysis of the CDV in diving state. (c) The movements of the CDV in a cross-domain process. (d) Force analysis of the CDV in floating state. (e) Force analysis of the CDV at high speed on water.

Table 1. The variable definitions.

Variable	Description
P	Thrust of water jet propeller
F	The resultant force of buoyancy and drag of the CDV
G	Gravity of the vehicle
F_f	Force of the front hydrofoil
F_r	Force of the rear hydrofoil
F_v	Force of the vertical-propeller
M	The moment of buoyancy
α	Included angle between F and the axial direction of CDV
β	Included angle between F_f and the axial direction of CDV
γ	Included angle between F_r and the axial direction of CDV
θ	Pitch angle
φ	Roll angle
$U_{i,j}$	The velocity component in the i and j directions
l_f	The distance from the front hydrofoil to the center of gravity
l_r	The distance from the rear hydrofoil to the center of gravity
l_v	The distance from the vertical-propeller to the center of gravity
J_k	The moment of the k axis

2.1. Dynamic Model of Surface State

The CDV has high-speed sailing capacity on the surface. When the CDV is sailing on the surface, the gravity is balanced by the lift force of the hydrofoil and the buoyancy force. The water jet propeller provides enough thrust to balance the drag. The heading motion of the CDV is realized by controlling the angle of the rudder. The rudder turns to the right at a certain angle to provide the moment that causes the vehicle to steer to the right. Similarly, the rudder turns to the left at an angle and the vehicle steers to the left. The vehicle can sail freely on the surface by controlling the thrust of the water jet propeller and the rudder.

When the CDV is sailing at high speed on the surface, the wet area and drag of the CDV decrease because the CDV is lifted by the hydrofoil.

When the CDV rolls clockwise, the wet area and lift force of the right hydrofoil increase, which produce a recovery moment. The CDV tends to return to its original attitude because of this recovery moment. Therefore, the CDV has self-stability due to the hydrofoil.

When the CDV sails on the surface, the force and moment distribution of the CDV are shown in Figure 2a,e. According to this, the linearized system model of the CDV is obtained,

$$m\ddot{U}_i = P\cos\theta - F\cos(\alpha - \theta) - F_f\cos(\beta - \theta) - F_r\cos(\gamma - \theta) \quad (1)$$

$$m\ddot{U}_j = F\sin(\alpha - \theta) + F_f\sin(\beta - \theta) + F_r\sin(\gamma - \theta) + P\sin\theta - G \quad (2)$$

$$J_k\ddot{\theta} = M + F_f l_f \sin\beta - F_r l_r \sin\gamma \quad (3)$$

where l_f and l_r are the distance from the front and rear hydrofoil to the center of gravity, respectively.

When navigating on the surface, the CDV will produce a pitch angle θ . The combined drag and lift forces of the front hydrofoil on the hull is F_f . β is the included angle between F_f and the axis direction of the CDV, which can be obtained by inverse trigonometric functions of the lift and the drag of the front hydrofoil. The F_r of the rear hydrofoil on the hull can be analyzed via a similar method. γ is the included angle between F_r and the axis of the CDV, which can be obtained by the inverse trigonometric function of the lift and the drag of the rear hydrofoil. The direction of the thrust of the water jet propeller is consistent with the axis of the CDV. The buoyancy force and the drag force of the hull produce a counterclockwise moment M and the angle between F and the axis direction of the CDV is α . The dynamic model of surface state can be used for the design of the CDV.

2.2. Dynamic Model of Underwater State

It is very important to adjust the gravity and buoyancy of the CDV for underwater navigation. On the water surface, the buoyancy of the CDV is almost equal to gravity. The underwater navigation of the CDV is realized by the upward and downward forces provided by the vertical propeller and the hydrofoil.

When the vertical propeller provides a downward force, the CDV generates a negative pitch angle and the hydrofoil generates the downward force. This results in less buoyancy of the CDV than gravity and the CDV dives. Figure 2b shows the distribution of the force and the moment when the CDV dives. The diving dynamic model of underwater state is obtained as follows,

$$m\ddot{U}_i = P\cos\theta - F\cos(\alpha + \theta) - F_f\cos(\beta - \theta) - F_r\cos(\gamma - \theta) \quad (4)$$

$$m\ddot{U}_j = F_v\cos\theta + F_f\sin(\beta - \theta) + F_r\sin(\gamma - \theta) + P\sin\theta + G - F\sin(\alpha + \theta) \quad (5)$$

$$J_k\ddot{\theta} = F_vl_v + F_f l_f \sin\beta - F_r l_r \sin\gamma - M \quad (6)$$

where m is the total weight of the CDV. \ddot{U}_i is the acceleration in the direction of axis i . \ddot{U}_j is the acceleration in the direction of axis j . J_k is the inertia moment of the vehicle around axis k . $\ddot{\theta}$ is the angular acceleration of the CDV. The pitch angle of the vehicle is managed by controlling F_v .

When the vertical propeller provides an upward force, the CDV generates a positive pitch angle and the hydrofoil generates an upward force. At this time, the upward force of the CDV is greater than the gravity and the CDV floats. The buoyancy and the drag of the CDV produce a counterclockwise moment M . Figure 2d shows the distribution of the force and the moment when the CDV floats. The floating dynamic model of the underwater state is obtained as follows,

$$m\ddot{U}_i = P\cos\theta - F\cos(\alpha - \theta) - F_f\cos(\beta - \theta) - F_r\cos(\gamma - \theta) - F_v\sin\theta \quad (7)$$

$$m\ddot{U}_j = F_v\cos\theta + F_f\sin(\beta - \theta) + F_r\sin(\gamma - \theta) + P\sin\theta + F\sin(\alpha + \theta) - G \quad (8)$$

$$J_k\ddot{\theta} = F_vl_v + F_f l_f \sin\beta + M - F_r l_r \sin\gamma \quad (9)$$

2.3. Underwater/Surface Transition State

The CDV needs to realize the underwater/surface transition, namely, entering the water and exiting the water. In general, the traditional UUV uses buoyancy adjustment equipment to achieve underwater/surface transition, but this is complex and difficult to control. Qianxiang I uses a vertical propeller to adjust the attitude of the CDV and four hydrofoils to provide upward or downward forces to realize the underwater/surface transition.

Figure 2a,b show the water entry process of the CDV. In this process, the vertical propeller generates a downward force. The pitch angle of the CDV changes from positive to negative. The force provided by the hydrofoils changes from upward to downward. The downward force of the CDV is greater than the buoyancy force. Finally, the CDV transitions from the surface to underwater.

Figure 2d,e show the water exit process of the CDV. In this process, the vertical propeller does not provide force. The pitch angle of the CDV gradually changes from negative to positive. The buoyancy force of the CDV is greater than gravity. As a result, the CDV transitions from underwater to the surface.

3. The Fabrication of the CDV

3.1. Overall Configuration of CDV

Based on concept and design principles, the CDV includes a vertical propeller, front hydrofoils, antenna section, permeable section, a rudder, rear hydrofoils, propeller section and stable rudders. The CDV has a gross weight of 45 kg, hull length of 2000 mm and

diameter of 200 mm. In order to enable the CDV to sail at high speed on the water surface, a pair of front hydrofoils and a pair of rear hydrofoils are installed at the front and rear of the CDV, respectively.

Figure 3 shows a perspective view and a physical view of the CDV. The hull shell is made of 8 mm wall-thickness aluminum alloy. The joints of different sections are sealed with sealing rubber rings and the water leakage detectors are installed in the antenna section and propeller section to detect whether there is water leakage.

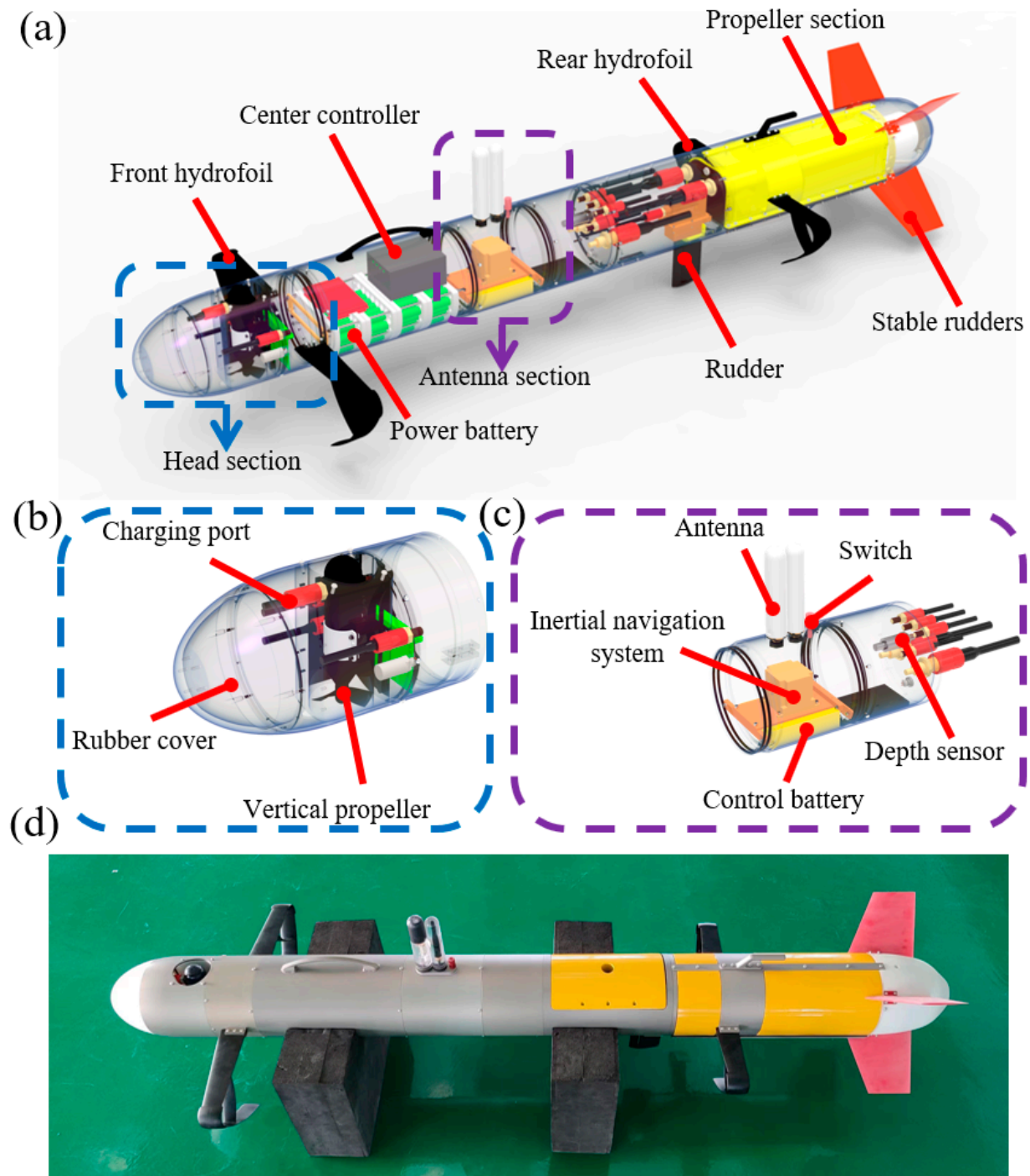


Figure 3. (a) The perspective view of the CDV. (b) The enlarged view of head section. (c) The enlarged view of antenna section. (d) The physical picture of the CDV.

The head section includes a charging port, rubber cover and vertical propeller, as shown in Figure 3b. The charging port charges the power and control batteries. The rubber cover can prevent the bow of the CDV from being damaged. The vertical propeller controls the diving and floating of the CDV. The power battery is located behind the head section and provides power for the water jet propeller. The total capacity of the power battery is 1200 Wh, which can meet the requirement that the CDV can sail for 10 h at a speed of 3 kn. The center controller is located above the power battery. This is like the brain of the CDV, receiving all the information and sending the mission instructions. The antenna section is located behind the power battery. The external part of the antenna section including three cylindrical parts: global navigation satellite system (GNSS) antenna, radio telemetry antenna and the power switch, as shown in Figure 3c. Their diameters are 32 mm, 32 mm and 15 mm and their heights are 160 mm, 160 mm and 25 mm. The internal part of the antenna section includes control battery, inertial navigation system (INS) and depth sensor, as shown in Figure 3c. The capacity of the control battery is 400 Wh, which can meet the requirements of the control system of the CDV for 15 h. The INS integrates the fiber optic inertial navigation and GNSS modules. The depth sensor is used to measure the depth of the CDV. The rudder is located at the bottom in the rear of the CDV. The propeller section is located at the rear of the CDV. The propeller section is wrapped by buoyant material and has a downward water inlet at the bottom of the CDV. The stable rudders are located at the rear of the propeller section. A physical view of the CDV is shown in Figure 3d.

Considering that the turning radius of the CDV should be as small as possible, the rudder is located on the rear part of the hull and its maximum torque is 12 N·m. The rudder airfoil is NACA0018, with a chord length of 80 mm and a span length of 130 mm. The stable rudders are designed as X-shaped to increase the stability of the CDV. To reduce the drag, the stable rudders are designed as NACA0010. The stable rudder has a span length of 150 mm, a root chord length of 100 mm and a contraction coefficient of 1.5. The material of the stable rudders is poly-ether-ether-ketone (PEEK).

3.2. Structural Design of Hydrofoil

Figure 4a shows the main structures of the hydrofoil, including flat wing, inclined wing and support wing. The front hydrofoils and rear hydrofoils have the same structure, but different dimensions.

The chord length of the front and rear hydrofoils is the same and the root chord length of the flat wing is 60 mm. The tip chord length of the flat wing is 45 mm. The chord length of the inclined wing is also 45 mm. The support wing is connected with the flat wing and the inclined wing to improve the strength of the hydrofoil. The span of the front hydrofoil is greater than that of the rear hydrofoil, which can increase the stability of the CDV.

The hydrofoil is subjected to a large impact force when the CDV is sailing at high speed on the water surface and the weight of the hydrofoil has a great influence on the diving and floating of the CDV. Therefore, the hydrofoil needs to have high structural strength on the basis of light weight. Here, the aviation aluminum alloy 7075 is used to make the hydrofoils.

For the structural design of hydrofoil, its pitch angle is controlled within the range of 0 to 6°. When the CDV is sailing at high speed on the surface, the lift force is mainly generated by the inclined wing. Therefore, the inclined wing of the hydrofoil needs to have a high lift drag ratio in the angle range of 0–6°. AG24 airfoil is used for inclined wing, which has a high lift drag ratio in the range of 0–6° [26], as shown in Figure 4b,c. In addition, when the CDV is navigating underwater, the drag of the CDV needs to be reduced. NACA0012 airfoil is used for the flat wing and support wing because of its drag-reduction capabilities, as shown in Figure 4b,c [27].

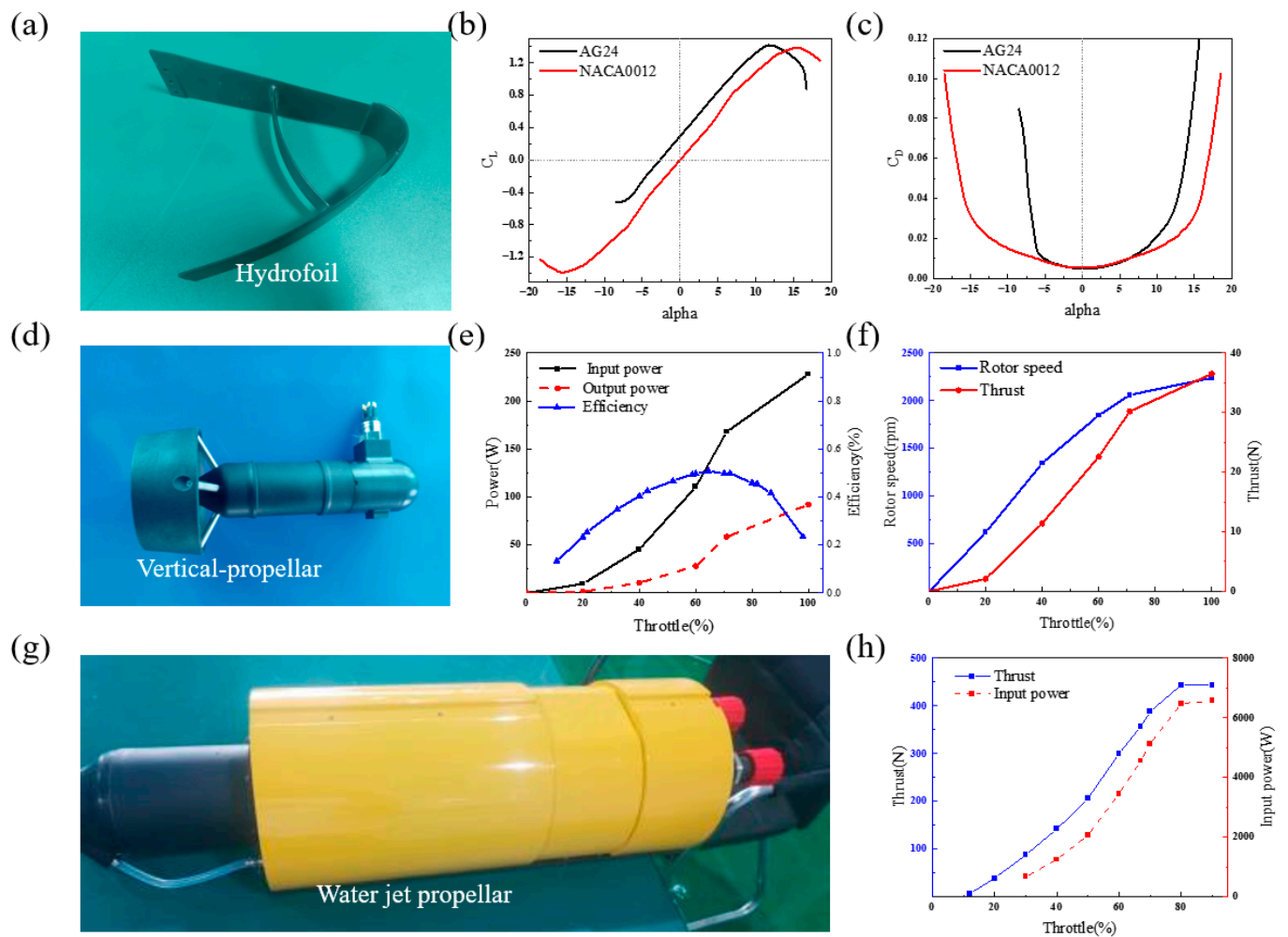


Figure 4. (a) Hydrofoil structure. (b,c) Lift and drag coefficient of the hydrofoil. (d) Vertical propeller. (e) Power and efficiency of vertical propeller. (f) Rotor speed and thrust of the vertical propeller. (g) Water jet propeller. (h) Input power and thrust of water jet propeller.

3.3. Propulsion System

The propulsion system of the Qianxiang I is composed of a water jet propeller and a vertical propeller. When the CDV is sailing at high speed on the water surface, the CDV needs to provide a large output of power and thrust. The water jet propeller has the characteristics of a simple transmission mechanism, low noise, good anti-cavitation performance and high efficiency at high speed. Therefore, the water jet propeller is a better choice for the propulsion of the CDV. The thrust and power of the water jet propeller are shown in Figure 4h. The maximum thrust of the water jet propeller is 440 N and the maximum power is 6500 W.

The vertical propeller is adopted in the bow of the vehicle, which is used to realize the floating and diving functions of the CDV. The vertical propeller uses a three-bladed propeller with a radius of 40 mm. The rotor speed and power of the vertical propeller are shown in Figure 4e,f. When the CDV is navigating underwater, the vertical propeller provides a maximum thrust of 35 N.

3.4. Avionics Control System

To make the internal structure of the CDV more compact, a modular design method is adapted. The avionics control system of the Qianxiang I is mainly divided into three subsystems, namely the energy supply system, propulsion control system and information processing system, as shown in Figure 5.

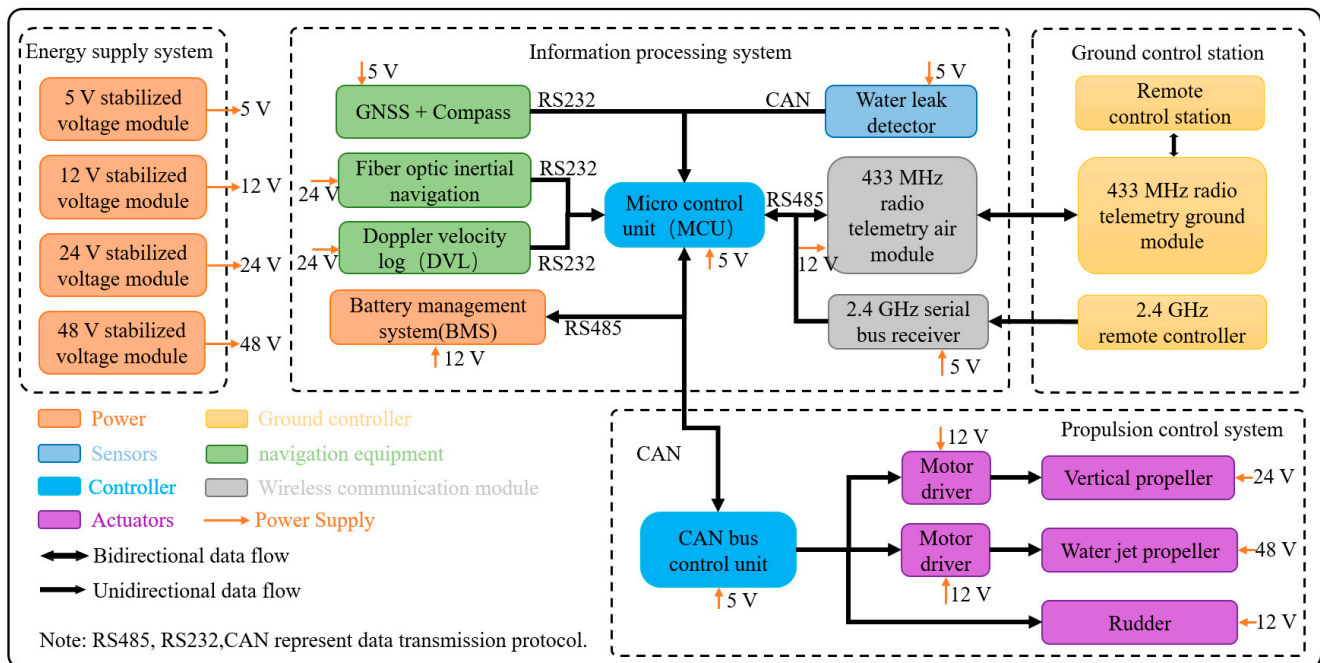


Figure 5. Schematic of the avionics control system.

The main function of the energy supply system is to supply power to each module. To ensure the stability of the energy supply system, the battery is divided into equipment battery and power battery. The capacity and output voltage of the equipment battery is 120 Wh and 25.2 V. The capacity and output voltage of the power battery is 1.2 kWh and 50.4 V. By four groups of voltage regulator modules, the voltage output of 5 V, 12 V, 24 V and 48 V can be obtained. Therefore, the energy supply system meets the requirements of supply voltage for different equipment and power systems (e.g., Micro control unit—5 V, fiber optic inertial navigation—24 V).

The propulsion control system mainly consists of a controller area network (CAN) bus control unit, two motor drivers, a vertical propeller for floating and diving control, a water jet propeller for speed control and a rudder for adjusting the heading angle. Through the unique CAN bus communication protocol, the CAN bus control unit receives the control information of the micro control unit (MCU), which can control two motor drivers to drive the vertical propeller and the water jet propeller. The rudder can be directly controlled through the CAN bus control unit without additional signal conversion.

The information processing system of the CDV mainly includes a MCU, a GNSS, an electronic compass, a fiber optic inertial navigation, a doppler velocity log (DVL), a 433 MHz radio telemetry air module, a 2.4 GHz serial bus receiver and water leakage detectors. A STM32F407 microcontroller is used as the core control system board of the MCU, which utilizes different communication interfaces (RS232, RS485) to receive different equipment information. In addition, the GNSS and the electronic compass are used to obtain the position and heading information of the CDV, respectively. The fiber optic inertial navigation is used to provide navigation information for underwater navigation. DVL is a sonar device that can obtain the actual navigation speed information by measuring the velocity relative to the water bottom. The water leakage detectors are distributed in each section of the CDV, which can effectively detect whether there is water leakage and send out warning signals in time. The 433 MHz radio telemetry air module is the main equipment for communication with the ground station and the 2.4 GHz serial bus receiver is mainly used to receive the signal for propulsion control in manual mode.

The ground control station is used to receive information from the avionics control system and provide remote control signals. The ground control station includes a remote control station, a 433 MHz radio telemetry ground module and a 2.4 GHz remote controller.

The remote control station communicates with the CDV through the 433 MHz radio telemetry ground module, which is used for real-time transmission of the tracking information, sensor information and equipment information. In addition, the remote control of the CDV can be realized through the 2.4 GHz remote controller in some specific cases (such as the DVL failure, 433 MHz wireless communication failure, etc.).

4. Performance Characterization of the CDV

In order to verify the feasibility of the CDV, it was tested in three states, surface state, underwater state and underwater/surface transition state, in Cangzhou, Hebei Province, China, from 1 September to 5 September 2022. The water area for testing the CDV is 200×300 m and the maximum water depth is 20 m. The wave height at water surface was about 0.05 m and the wind speed was about 3 m/s. An inertial navigation system with 4 Hz sampling frequency is used to measure the attitudes and speeds of the CDV. The measurement error of the inertial navigation system is less than 1%.

4.1. Surface Sailing

Figure 6 shows the velocity, roll and pitch of the CDV when it is sailing on the water surface with and without hydrofoils at 30% throttle. By adding hydrofoils to the CDV, the root mean square (RMS) of the fluctuation of the velocity reduces from 0.35 kn to 0.19 kn when the CDV is sailing stably on the water surface. Meanwhile, the RMS of the fluctuation of the pitch reduces from 0.74° to 0.03° . This shows that the stability of the CDV can be increased by adding hydrofoils. The results show that the speed of the CDV with hydrofoils is greater than that of the CDV without hydrofoils, which indicates that hydrofoils can reduce the drag of the CDV on the water surface.

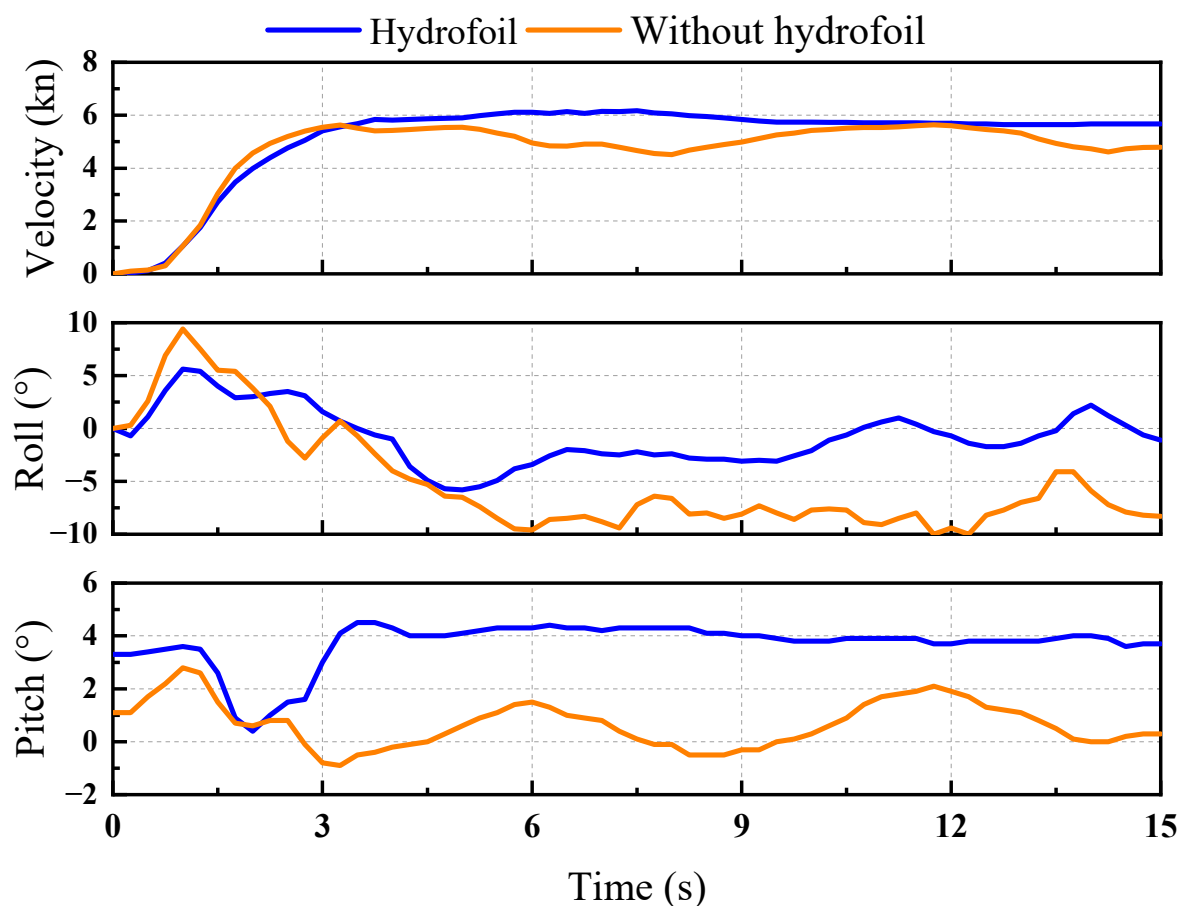


Figure 6. Surface sailing experiments with and without hydrofoils at 30% throttle.

Figure 7a shows the attitude of the CDV when it is sailing at high speed on the water surface at 50% throttle. Figure 7b shows the velocity, pitch and roll of the CDV during a high-speed sailing experiment on the water surface. The shaded part is the acceleration process. The sailing lasted for 15 s, which was divided into two stages: the acceleration stage and the stably sailing stage. The period from 0–5 s is the acceleration stage of the CDV, in which the CDV accelerates from stationary to maximum velocity. In this process, the pitch angle of the CDV increased to 4° and the roll angle fluctuated between $\pm 4^\circ$. The 6–15 s is the stably sailing stage and the maximum velocity of the CDV reaches 14 kn. During the stably sailing stage, the bow of the CDV is lifted out of the water by the hydrofoils, which greatly reduces the drag of the CDV. The velocity of the CDV fluctuates between 12 kn and 14 kn. The RMS values of the fluctuation of the velocity and pitch angle were 0.43 kn and 0.74° , respectively. In addition, the change amplitude of roll angle is greater than that of pitch angle. In general, the CDV can sail at high speed stably on the water surface.

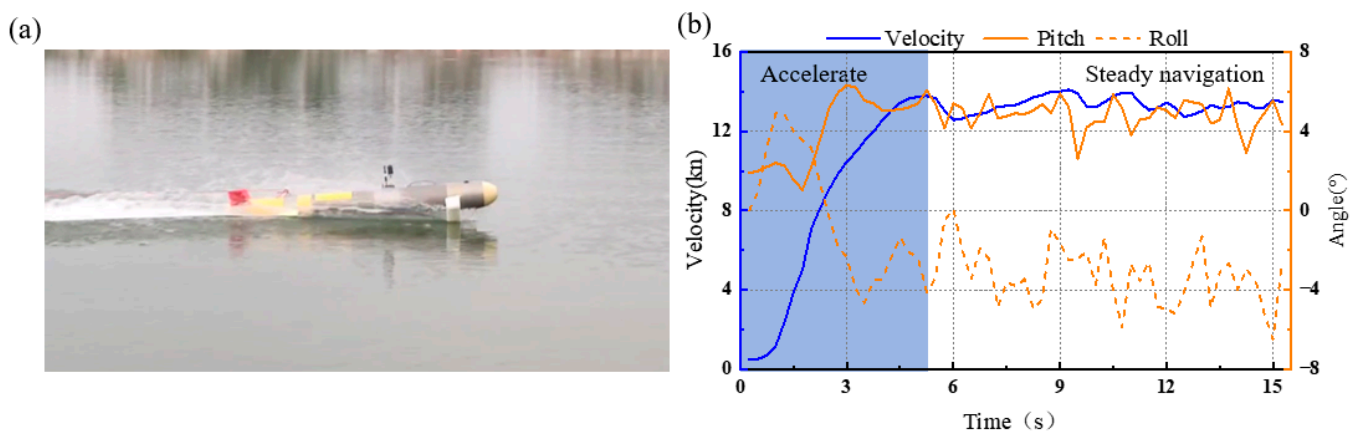


Figure 7. The experimental data of the CDV high speed sailing on the water surface at 50% throttle. (a) The photograph of the CDV at high speed; (b) The velocity, pitch and roll of the CDV at high speed sailing.

Figure 8 shows the attitude of the CDV during the acceleration stage on the water surface. In the initial state, the pitch angle of the CDV is 2° and the roll angle is 0° . The main part of the CDV is underwater and only the antenna is on the water. Within 0–2 s, when the CDV is at low speed, the bow of the CDV is submerged underwater as the lift provided by the front hydrofoil is insufficient to lift the CDV, as shown in Figure 8a–c. Within 2–4 s, the CDV produces a large amount of spray as the bow of the CDV impacts the water, as shown in Figure 8d–g. Within 4–5 s, the speed of the CDV increases gradually, as shown in Figure 8h,i. The bow of the CDV is lifted out of the water by the hydrofoil, which reduces the wet area of the CDV and thus reduces the drag. This is consistent with the expected effect of hydrofoil design.

The speed of CDV was compared with nine other vehicles, as shown in Table 2. While the speed of conventional vehicles is less than 5 kn, the CDV can reach a maximum speed of 14 kn.

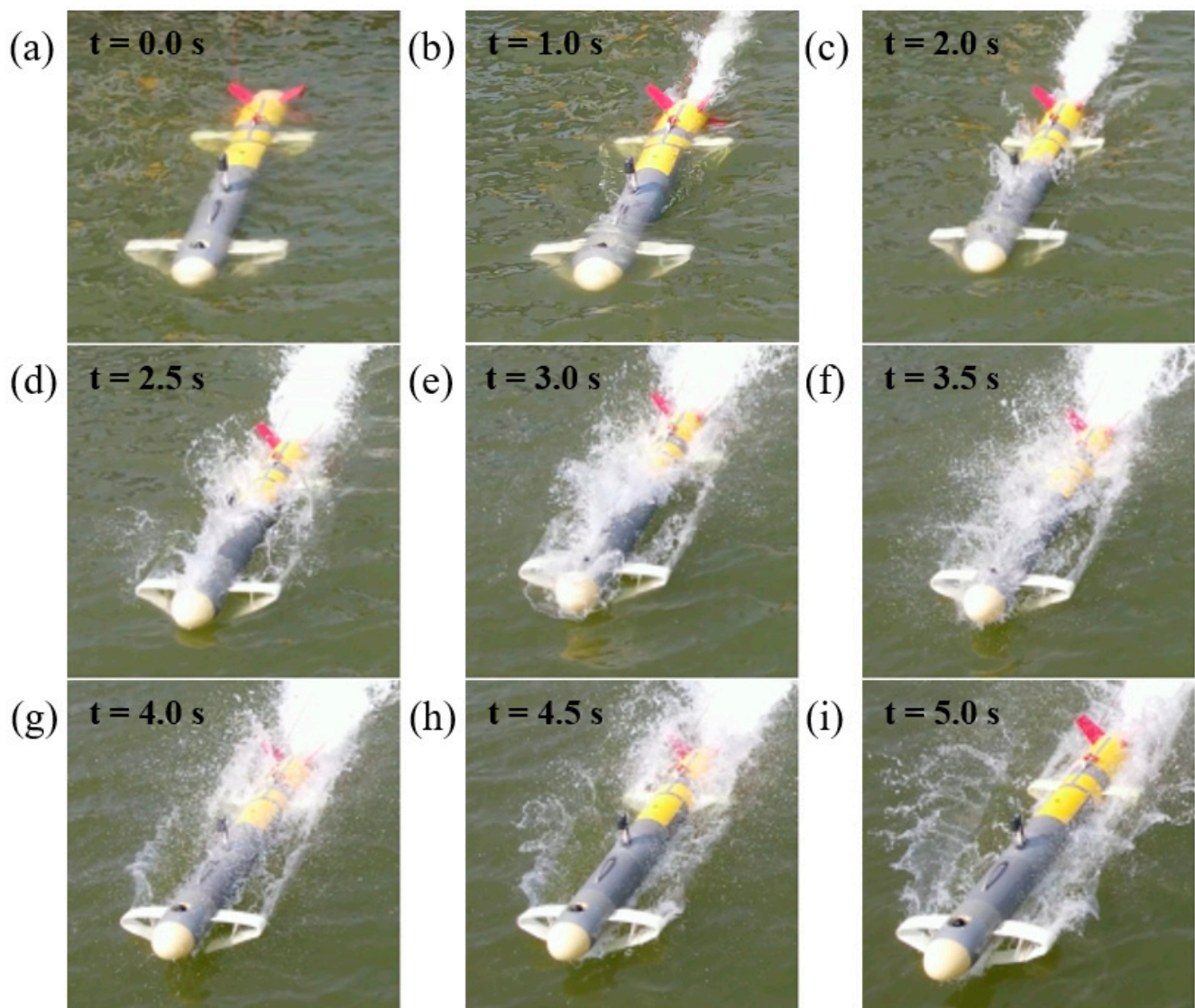


Figure 8. Photography of the attitude of the CDV during the acceleration stage on the water surface in the experiment. (a–i) The continuous photography of the CDV acceleration process.

Table 2. Comparison with different AUVs.

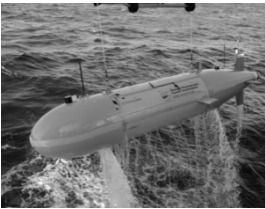
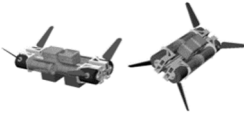





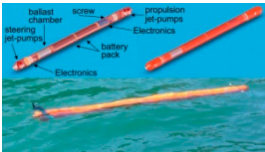

AUV Name	Development	Weight	Dimension	Depth	Endurance	Velocity
 Autosub6000 [28]	Southampton, UK	750 kg	3.5 m, dia 80 cm	6000 m	91 days	2 kn

Table 2. Cont.

AUV Name	Development	Weight	Dimension	Depth	Endurance	Velocity
 BFFAUV [29]	Massachusetts Institute of Technology, USA		2 m × 0.5 m × 0.5 m	10 m		4 kn
 Starbug [30]	Queensland, Australia	26 kg	1.2 m, dia 15 cm	100 m	4 h	3 kn
 Maya [31]	National Institute of Oceanography, India	54.7 kg	1.7 m, dia 23 cm	40 m	7.2 h	3 kn
 SPARUS II [32]	University of Girona, Spain	52 kg	1.6 m, dia 23 cm	200 m	10 h	4 kn
 Plateau data-gathering AUV [33]	Harbin Engineering University, China	96 kg	dia 28 cm	100 m		4 kn
 LoCO AUV [34]	University of Minnesota Computer Science, USA	12.5 kg	73 × 34 × 14 cm	100 m	2 h	3 kn
 Folaga [35]	Mediterranean Studies, Spain	30 kg	2 m, dia 14 cm	100 m	8 h	2 kn
 Qianxiang I	This paper	45 kg	2 m, dia 20 cm	10 m	10 h	14 kn

4.2. Underwater Navigating

In this section, the underwater navigation ability of the CDV was tested. In the experiment, the sampling interval is 0.25 s. The error of the depth sensor is 0.01 m. Since the vertical velocity cannot be measured directly, the vertical velocity is estimated by differentiating the curve of measured depth with time. According to the depth sensor error and sampling interval, the error of the estimated vertical velocity is 0.04 m/s. The estimated vertical velocity has obvious noise interference. In fact, the vertical velocity is continuous and stable. Therefore, the estimated vertical velocity is smoothed by the Savitzky-Golay method, which adopts the first-order polynomial and the number of windows is selected as 5 [36]. Then the vertical filter speed can be obtained by smoothing the estimated vertical velocity.

Figure 9a,b show the vertical speed, pitch and roll of the CDV for the fixed depth navigation experiment. During the fixed depth test of the CDV, the total navigation time is 140 s. The first stage is 0–28 s, in which the CDV dives from the water surface to the fixed depth of 1.5 m. In this process, the vertical velocity reaches a maximum value of -0.24 m/s and the pitch angle is negative. The second stage is 28–120 s, in which the CDV navigates steadily at the fixed depth. In this process, the depth of the vehicle gradually converges and finally stabilizes at the fixed depth. The pitch angle gradually converges and finally stabilizes at 0° . The third stage is 120–140 s, in which the CDV floats from the fixed depth to the water surface. In this process, the vertical velocity of the CDV is positive and the maximum value is 0.3 m/s. The pitch is positive and the maximum value is 15° . The roll angle is close to 0° . The experiment results show that the CDV can quickly dive to the fixed depth, stably navigate at the fixed depth and quickly float from the fixed depth to the water surface.

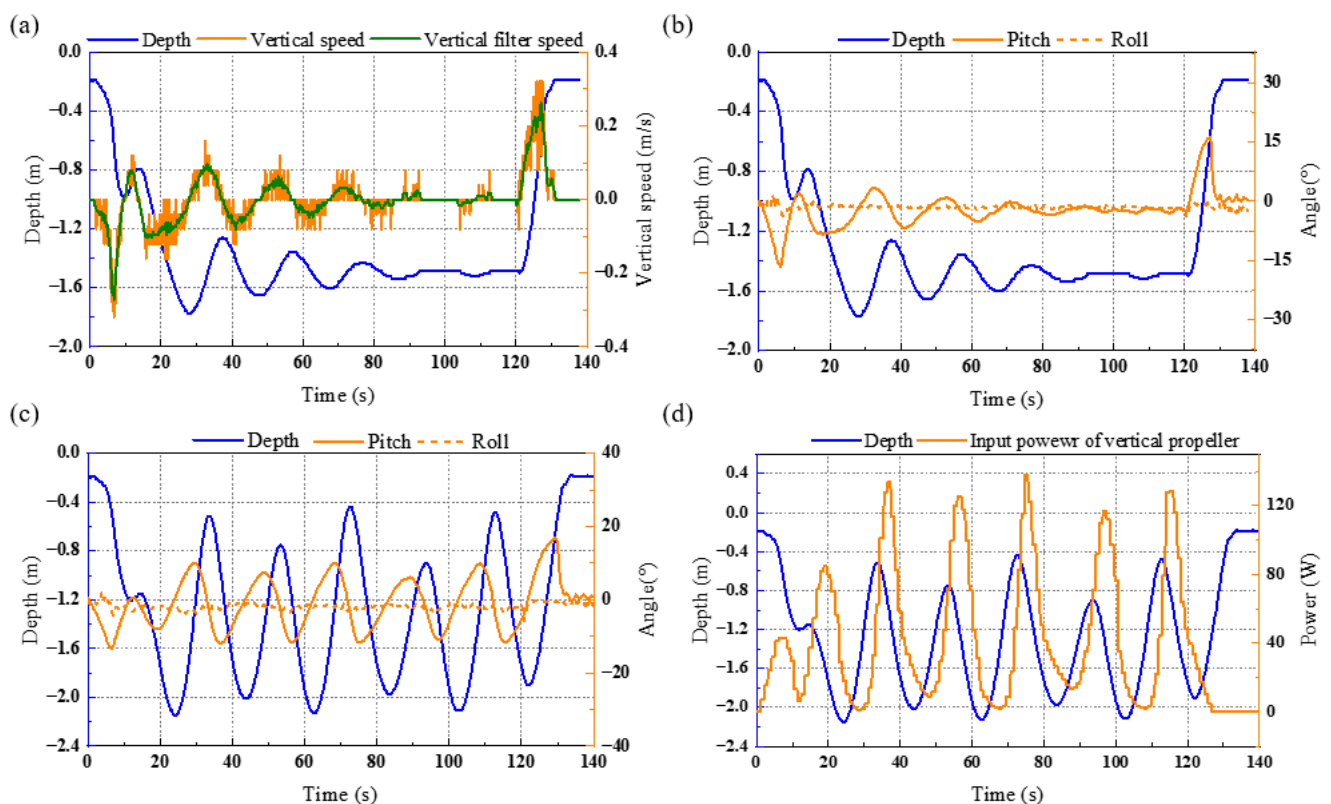


Figure 9. (a,b) The vertical speed, pitch and roll of the CDV for the fixed depth navigation experiment. (c,d) The input power of the vertical propeller, pitch and roll of the CDV when the CDV floats up and dives repeatedly.

Figure 9c,d show the input power of the vertical propeller, pitch and roll when the CDV floats up and dives repeatedly. The floating and diving of the CDV is controlled by the vertical propeller within the depth range of -0.4 m to -2.5 m. As the input power of the vertical propeller increases, the pitch angle of the CDV changes from positive to negative. When the pitch angle is negative, the CDV begins to dive and the depth increases. As the input power of the vertical propeller decreases, the pitch angle of the CDV changes from negative to positive and the CDV begins to float due to the buoyancy. In addition, the roll angle of the CDV is almost kept at 0° during the whole process of floating and diving. The experimental results show that the CDV can achieve floating and diving motion steadily.

4.3. Underwater/Surface Transition

The underwater/surface transition of the CDV is divided into two main processes. The first process is the water entry process, in which the CDV sails from the water surface to the underwater. The second process is the water exit process, in which the CDV navigates from the underwater to the water surface.

Before entering water, the pitch angle of the CDV is positive and small when it is sailing on the surface at low speed. In the water entry process, the vertical propeller provides a downward force that causes the bow of the CDV to dive. At the same time, the pitch angle of the CDV changes from positive to negative and the force on the hydrofoils changes from an upward lift to a downward lift. When the downward force is greater than the buoyancy, the CDV begins to dive. Figure 10a shows the continuous sequence of photos of the CDV entering the water during the experiment. In the water exit process, the pitch angle increases to a positive value as the input power of the vertical propeller decreases. The CDV begins to float up through its own buoyancy. Figure 10a shows the continuous sequence of photos of the CDV exiting the water during the experiment. The experimental results show that the CDV can realize the underwater/surface transition.

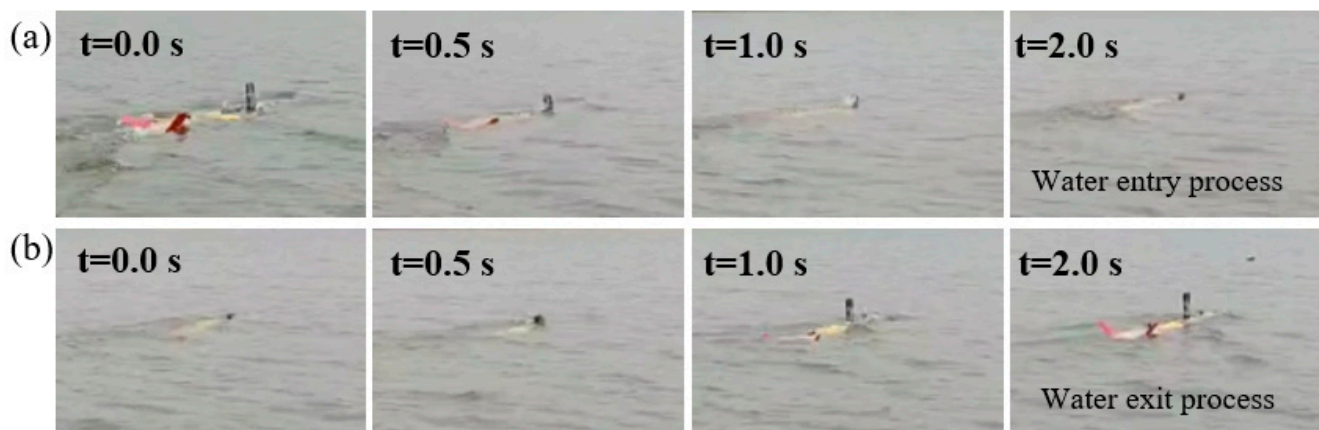


Figure 10. Photograph sequence of water entry and water exit process. (a) The continuous photography of CDV water entry process. (b) The continuous photography of CDV water exit process.

5. Discussion

In this paper, we designed a high speed CDV with hydrofoil. Through design, fabrication and experiments, the CDV showed excellent performance. In addition, we obtained many valuable research insights from the experimental results: (1) a hydrofoil structure with fixed degree may not be an optimal choice for the CDV. In the future, we will optimize the hydrofoil structure to increase the hydrodynamic performance of the CDV. (2) In the current experiment, the depth of the CDV is limited mainly by the water jet propeller. Therefore, we will further enhance the pressure resistance of the water jet propeller, so as to increase the submergence depth of the CDV. (3) At present, the stability of the CDV is achieved by the self-stability of the structure. In different mission scenarios, uncertain loads, which are caused by wind, wave and current, will affect the stability of the CDV.

In the future, we can improve the stability of the CDV at high speed by optimizing the control algorithm.

6. Conclusions

This paper presented the concept of the CDV, which was designed to perform underwater and with high-speed surface navigation. The design of the CDV has three properties, compared with traditional vehicles. First, a new hydrofoil is designed for high-speed navigation on the water surface. Second, a vertical propeller is used for the CDV, which can achieve diving and floating in the water. Third, a water jet propeller is used, which allows the CDV to navigate with high efficiency and low noise.

In this work, we designed and fabricated a cross-domain vehicle (CDV) that can both navigate at high speed on the surface like a USV and dive silently underwater like a UUV. The CDV's propulsion is provided by a water jet propeller and its dive is achieved by a vertical propeller. In addition, we designed a set of hydrofoils for the CDV, which greatly increased the surface speed to 14 kn and improved the navigation stability. The effects of the hydrofoils were tested in experiments, which showed that the hydrofoils improved the stability and surface sailing speed of the CDV. The performance of the CDV was experimentally characterized, proving the feasibility of the high-performance CDV and facilitating the understanding of the mechanism of the multi-state transition process.

Author Contributions: Conceptualization, K.L.; Data curation, Y.Z. and B.L.; Formal analysis, X.W.; Investigation, Y.W. and P.L.; Methodology, Z.S. and X.T.; Project administration, H.L.; Writing—review & editing, H.D. All authors have read and agreed to the published version of the manuscript.

Funding: This work is supported by the National Natural Science foundation of China (NSFC) under Grants No. 12293000, 12293001, 12202010, 12172006, 11988102, U2141251 and the Wenhai Program of the S&T Fund of Shandong Province for Pilot National Laboratory for Marine Science and Technology (Qingdao) (Grant No. 2021WHZZB2000).

Institutional Review Board Statement: Not applicable.

Informed Consent Statement: Not applicable.

Data Availability Statement: Not applicable.

Acknowledgments: The authors wish to thank the editors and anonymous reviewers for their valuable suggestions.

Conflicts of Interest: The authors declare no conflict of interest.

Abbreviations

The following abbreviations are used in this manuscript:

CDV	Cross-domain Vehicle
USV	Unmanned Surface Vehicle
UUV	Unmanned Underwater Vehicle
MCU	Microcontroller Unit
INS	Inertial Navigation System
CAN	Controller Area Network
GNSS	Global Navigation Satellite System

References

1. Paull, L.; Saeedi, S.; Seto, M.; Li, H. AUV navigation and localization: A review. *IEEE J. Ocean. Eng.* **2013**, *39*, 131–149. [[CrossRef](#)]
2. Zeng, Z.; Lyu, C.; Bi, Y.; Jin, Y.; Lu, D.; Lian, L. Review of hybrid aerial underwater vehicle: Cross-domain mobility and transitions control. *Ocean. Eng.* **2022**, *248*, 110840. [[CrossRef](#)]
3. Hwang, J.; Bose, N.; Fan, S. AUV adaptive sampling methods: A review. *Appl. Sci.* **2019**, *9*, 3145. [[CrossRef](#)]
4. Li, D.; Du, L. AUV trajectory tracking models and control strategies: A review. *J. Mar. Sci. Eng.* **2021**, *9*, 1020. [[CrossRef](#)]
5. Lu, D.; Xiong, C.; Zhou, H.; Lyu, C.; Hu, R.; Yu, C.; Zheng, Z.; Lian, L. Design, fabrication, and characterization of a multimodal hybrid aerial underwater vehicle. *Ocean. Eng.* **2021**, *219*, 108324.

6. Costa, D.; Palmieri, G.; Palpacelli, M.C.; Panebianco, L.; Scaradozzi, D. Design of a bio-inspired autonomous underwater robot. *J. Intell. Robot. Syst.* **2018**, *91*, 181–192. [\[CrossRef\]](#)
7. Kelasidi, E.; Liljebäck, P.; Pettersen, K.Y.; Gravdahl, J.T. Integral line-of-sight guidance for path following control of underwater snake robots: Theory and experiments. *IEEE Trans. Robot.* **2017**, *33*, 610–628. [\[CrossRef\]](#)
8. Daou, H.E.; Salumäe, T.; Chambers, L.D.; Megill, W.M.; Kruusmaa, M. Modelling of a biologically inspired robotic fish driven by compliant parts. *Bioinspiration Biomim.* **2014**, *9*, 016010. [\[CrossRef\]](#)
9. Mou, J.; He, Y.; Zhang, B.; Li, S.; Xiong, Y. Path following of a water-jetted USV based on maneuverability tests. *J. Mar. Sci. Eng.* **2020**, *8*, 354. [\[CrossRef\]](#)
10. Zhao, Y.; Qi, X.; Ma, Y.; Li, Z.; Malekian, R.; Sotelo, M.A. Path following optimization for an underactuated USV using smoothly-convergent deep reinforcement learning. *IEEE Trans. Intell. Transp. Syst.* **2020**, *22*, 6208–6220. [\[CrossRef\]](#)
11. Conte, G.; De Capua, G.P.; Scaradozzi, D. Designing the NGC system of a small ASV for tracking underwater targets. *Robot. Auton. Syst.* **2016**, *76*, 46–57. [\[CrossRef\]](#)
12. Shkurti, F.; Xu, A.; Meghjani, M.; Higuera, J.C.G.; Girdhar, Y.; Giguère, P.; Dey, B.B.; Li, J.; Kalmbach, A.; Prahacs, C.; et al. Multi-Domain monitoring of marine environments using a heterogeneous robot team. In Proceedings of the International Conference on Intelligent Robots and Systems, Vilamoura-Algarve, Portugal, 7–12 October 2012; pp. 1747–1753.
13. Ross, J.; Lindsay, J.; Gregson, E.; Moore, A.; Patel, J.; Seto, M. Collaboration of multi-domain marine robots towards above and below-water characterization of floating targets. In Proceedings of the International Symposium on Robotic and Sensors Environments, Ottawa, ON, Canada, 17–18 June 2019; pp. 1–7.
14. Jin, H.S.; Cho, H.; Lee, J.H.; Huang, J.F.; Kim, M.J.; Oh, J.Y.; Choi, H.S. Study on unmanned hybrid unmanned surface vehicle and unmanned underwater vehicle system. *J. Ocean. Eng. Technology.* **2020**, *34*, 475–480. [\[CrossRef\]](#)
15. Chen, H.; Li, J.; Xuan, Y.; Huang, X.; Zhu, W.; Zhu, K.; Shao, W. First Rocketsonde Launched from an Unmanned Semi-submersible Vehicle. *Adv. Atmos. Sci.* **2019**, *36*, 339–345. [\[CrossRef\]](#)
16. Olmos, S.; Lara, J.D.; Carrasco, P. Investigation of hydrodynamic lift & drag on an autonomous winged submarine using computational fluid dynamics. *Ocean. Eng.* **2019**, *186*, 106094.
17. Zheng, Y.; Dong, W.C. Hull form design and preliminary evaluation of a surface planning submersible ship. In Proceedings of the International Society of Ocean and Polar Engineering Conference, Rhodes, Greece, 17 June 2012.
18. Ueno, M. Hydrodynamic derivatives and motion response of a submersible surface ship in unbounded water. *Ocean. Eng.* **2010**, *37*, 879–890. [\[CrossRef\]](#)
19. Ueno, M.; Tsukada, Y.; Sawada, H. A prototype of submersible surface ship and its hydrodynamic characteristics. *Ocean. Eng.* **2011**, *38*, 1686–1695. [\[CrossRef\]](#)
20. Huo, C.; Dong, W.C. Critical conditions of hydrodynamic diving and surfacing for a submersible high speed craft. In Proceedings of the International Society of Ocean and Polar Engineering Conference, Busan, Korea, 15 June 2014.
21. Cong, H.A.; Yi, Z.B.; Xiao, P.G. Free-running tests on a self-propelled submersible multi-state vehicle model. *Ocean. Eng.* **2021**, *236*, 109575.
22. Acosta, A.J. Hydrofoils and hydrofoil craft. *Annu. Rev. Fluid Mech.* **1973**, *5*, 161–184. [\[CrossRef\]](#)
23. Garg, N.; Pearce, B.W.; Brandner, P.A.; Phillips, A.W.; Martins, J.R.; Young, Y.L. Experimental investigation of a hydrofoil designed via hydrostructural optimization. *J. Fluids Struct.* **2019**, *84*, 243–262. [\[CrossRef\]](#)
24. Budiyo, M.A.; Prawira, N.Y.; Dwiputra, H. Lift-to-drag ratio of the application of hydrofoil with variation mounted position on high-speed patrol vessel. *CFD Lett.* **2021**, *13*, 1–9. [\[CrossRef\]](#)
25. Suastika, K.; Silaen, A.; Aliffranda, M.H.N.; Hermawan, Y.A. Seakeeping analysis of a hydrofoil supported watercraft (hysuwac): A Case Study. *CFD Lett.* **2021**, *13*, 10–27. [\[CrossRef\]](#)
26. Martin, H.R.; Kimball, R.W.; Viselli, A.M.; Goupee, A.J. Methodology for wind/wave basin testing of floating offshore wind turbines. *J. Offshore Mech. Arct. Eng.* **2014**, *136*, 020905. [\[CrossRef\]](#)
27. Ohtake, T.; Nakae, Y.; Motohashi, T. Nonlinearity of the aerodynamic characteristics of NACA0012 aerofoil at low Reynolds numbers. *Jpn. Soc. Aero-Naut. Space Sci.* **2007**, *55*, 439–445.
28. Morice, C.; Veres, S.; McPhail, S. Terrain referencing for autonomous navigation of underwater vehicles. In Proceedings of the IEEE Oceans 2009-Europe, Bremen, Germany, 2 October 2009.
29. Licht, S.; Polidoro, V.; Flores, M.; Hover, F.S.; Triantafyllou, M.S. Design and projected performance of a flapping foil AUV. *IEEE J. Ocean. Eng.* **2004**, *29*, 786–794. [\[CrossRef\]](#)
30. Dunbabin, M.; Roberts, J.; Usher, K.; Winstanley, G.; Corke, P. A hybrid AUV design for shallow water reef navigation. In Proceedings of the International Conference on Robotics and Automation, Barcelona, Spain, 10 January 2006.
31. Desa, E.; Madhan, R.; Maurya, P.; Navelkar, G.; Mascarenhas, A.; Prabhudesai, S.; Afzulpurkar, S.; Bandodkar, S. The small maya auv-initial field results. *Ocean. Syst. Eng.* **2007**, *11*, 6–9.
32. Carreras, M.; Candela, C.; Ribas, D.; Angelos, M.; Lluís, M.; Eduard, V.; Narcís, P.; Pere, R. Sparus II, design of a lightweight hovering AUV. In Proceedings of the Martech 2013 5th International Workshop on Marine Technology, Girona, Spain; 2013.
33. Xu, H.; Zhang, G.C.; Sun, Y.S.; Pang, S.; Ran, X.R.; Wang, X.B. Design and experiment of a plateau data-gathering AUV. *J. Mar. Sci. Eng.* **2019**, *7*, 376. [\[CrossRef\]](#)

34. Edge, C.; Enan, S.S.; Fulton, M.; Jungseok, H.; Jiawei, M.; Kimberly, B.; Hunter, B.; Berik, K.; Corey, K.; Kevin, O.; et al. Design and experiments with LoCO AUV: A low cost open-source autonomous underwater vehicle. In Proceedings of the International Conference on Intelligent Robots and Systems, Vegas, NV, USA, 10 February 2021.
35. Alvarez, A.; Caffaz, A.; Caiti, A.; Casalino, G.; Gualdesi, L.; Turetta, A.; Viviani, R. Folaga: A low-cost autonomous underwater vehicle combining glider and AUV capabilities. *Ocean. Eng.* **2009**, *36*, 24–38. [[CrossRef](#)]
36. Press, W.H.; Teukolsky, S.A. Savitzky-Golay smoothing filters. *Comput. Phys.* **1990**, *4*, 669–672. [[CrossRef](#)]

Disclaimer/Publisher’s Note: The statements, opinions and data contained in all publications are solely those of the individual author(s) and contributor(s) and not of MDPI and/or the editor(s). MDPI and/or the editor(s) disclaim responsibility for any injury to people or property resulting from any ideas, methods, instructions or products referred to in the content.